

DMD#78543

**Title Page**

***N*-acetyltransferase 2 Genotype-dependent *N*-acetylation of Hydralazine  
in Human Hepatocytes**

Cecily E. Allen, Mark A. Doll, and David W. Hein

*Department of Pharmacology & Toxicology and James Graham Brown Cancer Center*

*University of Louisville School of Medicine, Louisville, Kentucky*

DMD#78543

## Running Title Page

**Running Title:** Genotype-dependent hydralazine *N*-acetylation in hepatocytes

### Corresponding Author:

David W. Hein, Kosair Charities CTR-Room 303, 505 South Hancock Street, Louisville, KY  
40202. Telephone: 502-852-6252; (no fax number); Email: [d.hein@louisville.edu](mailto:d.hein@louisville.edu);

Number of text pages:

Number of tables: 0

Number of figures: 6

Number of references: 25

Number of words in Abstract: 224

Number of words in Introduction: 451

Number of words in Discussion: 703

Nonstandard abbreviations used: NAT1, *N*-acetyltransferase 1; NAT2, *N*-acetyltransferase 2;

MTP, 3-methyl-s-triazolo [3,4a]-phthalazine.

DMD#78543

## Abstract

Hydralazine is used in treatment of essential hypertension and is under investigation for epigenetic therapy in the treatment of neoplastic and renal diseases. *N*-acetyltransferase 2 (NAT2) exhibits a common genetic polymorphism in human populations. Following recombinant expression in yeast, human NAT2 exhibited an apparent  $K_m$  ( $20.1 \pm 8.8 \mu\text{M}$ ) for hydralazine over 20-fold lower than the apparent  $K_m$  ( $456 \pm 57 \mu\text{M}$ ) for recombinant human NAT1 ( $p=0.0016$ ). The apparent  $V_{max}$  for recombinant human NAT1 ( $72.2 \pm 17.9$  nmoles acetylated/min/mg protein) was significantly ( $p=0.0245$ ) lower than recombinant human NAT2 ( $153 \pm 15$  nmoles acetylated/min/mg protein) reflecting 50-fold higher clearance for recombinant human NAT2. Hydralazine *N*-acetyltransferase activities exhibited a robust acetylator gene dose-response in cryopreserved human hepatocytes both *in vitro* and *in situ*. Hydralazine *N*-acetyltransferase activities *in vitro* differed significantly with respect to NAT2 genotype at 1000  $\mu\text{M}$  ( $p=0.0319$ ); 100  $\mu\text{M}$  ( $p=0.002$ ); and 10  $\mu\text{M}$  hydralazine ( $p=0.0029$ ). Hydralazine *N*-acetyltransferase activities differed significantly ( $p<0.001$ ) among slow acetylator hepatocytes, ( $\text{NAT2}^*5\text{B}/^*5\text{B} > \text{NAT2}^*5\text{B}/^*6\text{A} > \text{NAT2}^*6\text{A}/^*6\text{A}$ ). The *in situ* hydralazine *N*-acetylation rates differed significantly with respect to NAT2 genotype following incubation with 10  $\mu\text{M}$  ( $p=0.002$ ) or 100  $\mu\text{M}$  ( $p=0.0015$ ) hydralazine and were higher following incubation with 100  $\mu\text{M}$  (10-fold) than 10  $\mu\text{M}$  (4.5-fold) hydralazine. Our results clearly document NAT2 genotype-dependent *N*-acetylation of hydralazine in human hepatocytes, suggesting that hydralazine efficacy and safety could be improved by NAT2 genotype-dependent dosing strategies.

DMD#78543

## Introduction

Hydralazine has been used for decades in the treatment of hypertension and is indicated in the long-term therapy of essential hypertension, in the short-term therapy of pregnancy-induced hypertension and eclampsia, and in the therapy of hypertensive crisis (Cohn et al., 2011). Hydralazine is one of the first line anti-hypertensive agents used to treat severe hypertension in pregnancy (Magee et al., 2003). More recently, hydralazine also has been shown to attenuate progression of chronic kidney disease (Tampe et al., 2015).

Hydralazine is currently in clinical trials in combination with valproate for epigenetic cancer therapy (reviewed in Dueñas-Gonzalez et al., 2014). Methylation at CpG regions in DNA promoters is a common alteration of neoplastic cells leading to uncontrolled proliferation via suppression of tumor suppressor genes. Hydralazine is a non-nucleoside inhibitor of DNA methylation (Chuang et al., 2005; Segura-Pacheco et al., 2006; Singh et al., 2009; 2013; Castillo-Aguilera et al., 2017). Studies have demonstrated hydralazine's ability to increase sensitivity to chemotherapeutics, decrease expression of cell cycle genes, increase DNA damage, and result in growth inhibition mediated through EGF signaling pathways (Coronel et al., 2011; Graca et al., 2014; Castillo-Aguilera et al., 2017).

Arylamine *N*-acetyltransferase 1 (NAT1) and 2 (NAT2) catalyze the *N*-acetylation of hydrazine and numerous arylamine drugs/xenobiotics (reviewed in Hein, 2009). As NAT2 is expressed mainly in the liver and gastrointestinal tract, it is often involved in drug metabolism (McDonagh et al., 2014). NAT2 expresses common genetic polymorphisms in human populations resulting in rapid, intermediate, and slow acetylator phenotypes (Hein, 2009). Previous studies showed 15-fold differences in hydralazine plasma concentrations between rapid and slow

DMD#78543

acetylators of the probe drug sulfamethazine following administration of the same dose of hydralazine (Shepherd et al., 1981). Since acetylator phenotype has been shown to modify plasma levels of hydralazine, acetylator phenotype or genotype-dependent dosing strategies have been both suggested and implemented (described further in the discussion).

*N*-acetylation of hydralazine generates an unstable *N*-acetylated intermediate that spontaneously converts to 3-methyl-s-triazolo [3,4a]-phthalazine (MTP) (reviewed in Weber and Hein, 1985). Although the differential plasma levels of hydralazine in rapid and slow acetylators strongly implicate an important role for NAT2 in hydralazine metabolism, the possible role of NAT1 and the comparative affinity of hydralazine for *N*-acetylation via NAT1 or NAT2 has not been reported.

The purposes of the present study were to 1) assess the relative ability and affinity of human NAT1 or NAT2 to catalyze the *N*-acetylation of hydralazine and 2) investigate the role of NAT2 genotype on *N*-acetylation rates both *in vitro* and *in situ* in cryopreserved human hepatocytes. The results are important for refinement of hydralazine dosing strategies, particularly in clinical trials investigating its possible efficacy as an epigenetic drug in the treatment of neoplastic and renal diseases.

DMD#78543

## Materials and Methods

**Production of Recombinant Human *N*-acetyltransferases.** The coding regions of *NAT1*\*4 (reference *NAT1*) and *NAT2*\*4 (reference *NAT2*) were amplified by polymerase chain reaction (PCR) using previously constructed plasmids as previously described (Hein and Doll, 2017). The yeast vector pESP-3 (Stratagene, La Jolla, CA) was digested with NdeI and AscI at 37°C overnight and gel purified. Purified PCR products and 80 ng of plasmid were ligated overnight at 16°C with T4 DNA ligase (New England Biolabs, Inc, Beverly, MA). Ligated plasmids were transformed into XL-10 Gold Ultracompetent *Escherichia coli* (Stratagene). Plasmids were isolated from cultures grown from selected colonies using the Qiagen Plasmid Midi kit (Qiagen, Valencia, CA) and sequenced using Thermosequenase (Amersham, Arlington Heights, IL). Constructs were then transformed into competent *Schizosaccharomyces pombe* and expressed following the manufacturer's instructions (Stratagene). Mock transformed yeast used pESP-3 vector with no *NAT2* insert. Total cell lysates were prepared by vigorous agitation of yeast in ice-cold 20 mM NaPO<sub>4</sub>, 1 mM dithiothreitol, 1 mM EDTA, 0.2% triton-X-100, 1 mM phenylmethylsulfonyl fluoride, 1 μM pepstatin A, and 1 μg/mL aprotinin containing acid-washed glass beads (Stratagene) for ten minutes at 4°C. Liquid fractions were collected from the lysed cells and centrifuged at 13,000 *x g* for twenty minutes. Supernatants were collected, aliquoted, and stored at -70°C until utilized for enzymatic assays. To mitigate possible instability of human *NAT1* and *NAT2*, supernatant aliquots were thawed only once and used immediately to carry out the enzymatic reactions. Apparent V<sub>max</sub> and apparent K<sub>m</sub> were determined by nonlinear regression of the Michaelis–Menten equation (GraphPad Software, Inc, San Diego, CA). Protein concentrations were determined using the Bio-Rad protein assay kit (Bio-Rad, Richmond, CA).

DMD#78543

**Source and Processing of Cryopreserved Human Hepatocytes.** Cryopreserved human hepatocytes were received from Bioreclamation IVT, (Baltimore, MD) and stored in liquid nitrogen until use. Upon removal from liquid nitrogen, hepatocytes were thawed according to the manufacturer's instructions by warming a vial of the hepatocytes at 37°C for 90 seconds and transferring to a 50 mL conical tube containing 45 mL of InVitroGRO HT medium (Bioreclamation IVT). The suspension was centrifuged at 50 x g at room temperature for 5 min. The supernatant was discarded and cells washed once in ice-cold PBS before lysing the cells in ice-cold 20 mM NaPO<sub>4</sub>, 1 mM dithiothreitol, 1 mM EDTA, 0.2% triton-X-100, 1 mM phenylmethylsulfonyl fluoride, 1 μM pepstatin A, and 1 μg/mL aprotinin. The lysate was centrifuged at 15,000 x g for 20 min and the supernatant was aliquoted and stored at -70°C. To mitigate possible instability of human NAT1 and NAT2, supernatant aliquots were thawed only once and used immediately to carry out the enzymatic reactions.

**Determination of NAT2 Genotype and Deduced Phenotype.** Genomic DNA was isolated from pelleted cells prepared from human cryopreserved hepatocyte samples as described above using the QIAamp DNA Mini Kit (QIAGEN, Valencia, CA) according to the manufacturer's instructions. NAT2 genotypes and deduced phenotypes were determined as described previously (Doll and Hein, 2001). Controls (no DNA template) were run to ensure that there was no amplification of contaminating DNA.

**Measurement of Hydralazine N-Acetyltransferase Activity *In Vitro*.** N-acetyltransferase assays containing yeast or hepatocyte lysate (<2 mg of protein/ml), 10 - 1000 μM hydralazine and 1 mM acetyl coenzyme A were incubated at 37°C. Reactions were terminated by the addition of 1/10 volume of 1 M acetic acid and the reaction tubes were centrifuged in a small biofuge at 15,000 x g for 10 minutes to precipitate protein. The amount of acetyl-hydralazine produced (measured

DMD#78543

as MTP) was determined following separation and quantitation by high performance liquid chromatography (HPLC). Separation of hydralazine and MTP was accomplished by injection (40  $\mu$ L) onto a 125 x 4 mm Lichrospher 100 RP-100 5 $\mu$ M C18 HPLC column subjected to a gradient of 100% 20 mM sodium perchlorate pH 2.5/0% acetonitrile to 50% 20 mM sodium perchlorate pH 2.5/50% acetonitrile over 5 min. Hydralazine and MTP eluted at 3.58 and 4.98 min respectively (Fig. 1). The intra-assay HPLC coefficient of variation was 2.56% for hydralazine and 1.66% for MTP with an MTP limit of detection of 100 pmoles/40  $\mu$ L. Protein concentrations were determined using the Bio-Rad protein assay kit (Bio-Rad, Richmond, CA).

Cryopreserved human hepatocytes were selected at random with rapid genotypes *NAT2*\*4/\*4 (n=6; (3 males and 3 females); intermediate genotypes *NAT2*\*4/\*5B (n=3), *NAT2*\*4/\*6A (n=2); (3 males and 2 females) and slow genotypes *NAT2*\*6A/\*6A (n=2), *NAT2*\*6A/\*7B (n=1), *NAT2*\*5B/\*5B (n=1), and *NAT2*\*5B/\*6A (n=1); (4 males and 1 gender unknown). To further explore genetic heterogeneity in the slow acetylator genotype, additional assays were conducted with 300  $\mu$ M hydralazine and 1 mM acetyl coenzyme A in cryopreserved human hepatocytes with genotypes *NAT2*\*5/\*5 (n=5; 3 males and 2 females), *NAT2*\*5/\*6 (n=6; 3 males and 3 females), and *NAT2*\*6/\*6 (n=5; 3 males and 2 females).

**Measurement of Hydralazine N-Acetylation *In Situ*.** Cryopreserved human hepatocytes previously identified as rapid, intermediate, or slow *NAT2* acetylator genotypes (Doll et al., 2017) were thawed as described above and transferred to 50 mL conical tubes containing 12 mL of InVitroGRO CP media. One mL of hepatocyte/media mixture was transferred to each well of 12 well Biocoat® collagen coated plates to allow cells to attach for 48 hours at 37°C. Following culture in growth media for 48 hours, the cells were washed 3 times with 500  $\mu$ L 1X PBS and replaced with PBS + dextrose and hydralazine concentrations from 7.8 to 1000  $\mu$ M. Hepatocytes

DMD#78543

were incubated for up to 12 hours after which media was removed and protein precipitated by addition of 1/10 volume of 1 M acetic acid. Media was centrifuged at 15,000 x g for 10 min and supernatant used to separate and quantitate hydralazine and MTP by HPLC as described above. Cell number was determined after 12 hours incubation with hydralazine and activity was calculated in nmoles of acetylated product /12h/million cells in rapid genotypes *NAT2\*4/\*4* (n=5); (2 males and 3 females); intermediate genotypes *NAT2\*4/\*5B* (n=4); *NAT2\*4/\*6A* (n=1); (2 males; 1 female; and 2 gender unknown) and slow genotypes *NAT2\*5B/\*6A* (n=2); *NAT2\*5B/\*5B* (n=2); and *NAT2\*6A/\*6A* (n=1); (4 males and 1 gender unknown).

**Statistical Analysis.** Differences in *N*-acetylation rates among rapid, intermediate, and slow *NAT2* acetylator genotypes were tested for significance by one-way analysis of variance followed by Tukey-Kramer multiple comparisons test (GraphPad Software, Inc, San Diego, CA).

DMD#78543

## Results

**Michaelis-Menten Kinetic Constants for Hydralazine *N*-Acetylation Catalyzed by Recombinant Human NAT1 and NAT2.** Apparent  $K_m$  and  $V_{max}$  were calculated for human recombinant NAT1 and NAT2 (Fig. 2). Following recombinant expression in yeast, human NAT2 exhibited an apparent  $K_m$  ( $20.1 \pm 8.8 \mu\text{M}$ ) over 20-fold lower than the apparent  $K_m$  ( $456 \pm 57 \mu\text{M}$ ) for recombinant human NAT1 ( $p=0.0016$ ). The apparent  $V_{max}$  for recombinant human NAT1 ( $72.2 \pm 17.9$  nmoles acetylated/min/mg protein) was significantly ( $p=0.0245$ ) lower than for recombinant human NAT2 ( $153 \pm 15$  nmoles acetylated/min/mg protein) which reflects 50-fold higher clearance for recombinant human NAT2 than NAT1.

**Hydralazine *N*-Acetyltransferase Activity *In Vitro* from Cryopreserved Human Hepatocytes.** Hydralazine *N*-acetyltransferase activities exhibited a robust and significant acetylator gene dose-response *in vitro* from human cryopreserved human hepatocytes. At concentrations of hydralazine ranging from 10 to 1000  $\mu\text{M}$ , the hydralazine *N*-acetyltransferase activities differed significantly between NAT2 acetylator phenotypes at 1000  $\mu\text{M}$  ( $p=0.0319$ ), 100  $\mu\text{M}$  ( $p=0.002$ ), and 10  $\mu\text{M}$  hydralazine ( $p=0.0029$ ). Highest levels were observed in rapid acetylator, lower levels in intermediate acetylator, and lowest levels in slow acetylator hepatocytes (Fig. 3). Mean hydralazine *N*-acetyltransferase activities in the intermediate acetylators were very similar to the arithmetic average between the rapid and slow acetylators at each hydralazine concentration.

Genetic heterogeneity was observed among slow acetylator genotypes. Hydralazine *N*-acetyltransferase activities differed significantly ( $p<0.001$ ) among the slow acetylator hepatocytes. Highest levels ( $1.74 \pm 0.29$  nmoles MTP/min/mg) in NAT2\*5B/\*5B, lower levels ( $0.704 \pm 0.142$

DMD#78543

nmoles MTP/min/mg) in *NAT2\*5B/\*6A*, and lowest levels ( $0.367 \pm 0.145$  nmoles MTP/min/mg) in *NAT2\*6A/\*6A* hepatocytes (Fig. 4).

**Hydralazine *N*-acetylation *in situ* in Cryopreserved Human Hepatocytes.** Hydralazine was unstable in various culture media but stable in phosphate-buffered saline (PBS) as measured by HPLC. Therefore, after plating hepatocytes in the normal growth media for 48 hours, hepatocytes were washed with PBS and incubated with PBS + dextrose when adding hydralazine. Under these conditions, *in situ* hydralazine *N*-acetylation in cryopreserved human hepatocytes was both concentration- and time-dependent (Fig. 5). Hydralazine *N*-acetylation rates differed significantly between rapid, intermediate, and slow acetylator hepatocytes following incubation with 10  $\mu$ M ( $p=0.002$ ) or 100  $\mu$ M ( $p=0.0015$ ) hydralazine with highest levels in rapid acetylator, lower levels in intermediate acetylator, and lowest levels in slow acetylator cryopreserved human hepatocytes (Fig. 6). Differences in the means for hydralazine *N*-acetylation rates between homozygous rapid and slow acetylators were higher following incubation with 100  $\mu$ M (10-fold) than 10  $\mu$ M (4.5-fold) hydralazine.

DMD#78543

## Discussion

As recently reviewed (McDonagh et al., 2014), hydralazine treatment for hypertension and resistant hypertension is affected by acetylator phenotype. In early studies in patients with hypertension, hydralazine plasma concentrations varied as much as 15-fold among individuals reflecting an “acetylator index” in the *N*-acetylation of the probe drug (sulfamethazine) used to determine acetylator phenotype (Shepherd et al., 1981).

More recently, hydralazine plasma levels were evaluated in 26 healthy volunteers (13 slow, 0 intermediate, and 13 rapid acetylators) after a single oral dose of 182 mg of a controlled-release hydralazine tablet (Gonzalez-Fierro et al., 2011). Hydralazine area under the curve plasma levels were 2.2-fold higher in slow than in rapid acetylators, which subsequently has been used as rationale for prescribing hydralazine doses 2.2-fold lower in slow (83 mg) than rapid (182 mg) acetylators. This dose adjustment yielded similar plasma levels of hydralazine in rapid and slow acetylators in several studies (Arce et al., 2006; Gonzalez-Fierro et al., 2011; Garces-Eisele et al., 2014) with at least one exception in a study from the same group (Candelaria et al., 2007). Although none of these studies measured MTP levels, they appear to be the experimental basis for clinical trials using a hydralazine dosing strategy of 83 mg in slow and 183 mg in rapid acetylators (either alone or in combination with other drugs such as valproic acid) for the epigenetic treatment of cancer. A dosing strategy for intermediate acetylators is not stated.

In a recent study (Spinasse et al., 2014), DNA samples from 169 patients with resistant hypertension treated with hydralazine were identified as rapid (12.4%), intermediate (38.5%) and slow (35.5%) acetylators (13.6% indeterminate) as deduced from NAT2 genotype. In this group of patients treated with hydralazine, only slow acetylators had significant blood pressure

DMD#78543

reductions although they also had a higher incidence of adverse effects; neither hydralazine nor MTP plasma levels were reported.

Following recombinant expression in yeast, we confirmed that NAT2 is the primary *N*-acetyltransferase responsible for acetylation of hydralazine at therapeutic concentrations based on the lower apparent  $K_m$ , signifying increased affinity, and the higher apparent  $V_{max}$  leading to a 50-fold higher hydralazine *N*-acetylation clearance by NAT2 than NAT1.

We investigated the *N*-acetylation of hydralazine in cryopreserved human hepatocytes from rapid, intermediate, and slow acetylators. Key findings in our study support a three-tier “tri-modal” acetylating variation, with phenotypic differences observed between rapid, intermediate, and slow NAT2 genotypes. Although we observed overlap in hydralazine *N*-acetylation rates among the NAT2 rapid, intermediate, and slow acetylator genotypes, nevertheless *N*-acetylation of hydralazine was NAT2 genotype-dependent with relative magnitude of differences between acetylator phenotypes dependent upon hydralazine concentration (and presumably on hydralazine dosing regimen). The Michaelis-Menten kinetic analysis of human NAT1 and NAT2 following recombinant expression in yeast suggest that NAT1 may contribute to the *N*-acetylation of hydralazine, particularly at higher hydralazine concentrations. Thus, the role of NAT2 genotype on hydralazine efficacy and toxicity may be greater following lower dosing regimens. Furthermore, we observed small but highly significant ( $p < 0.001$ ) differences among slow acetylator genotypes supporting the concept of an acetylating index as previously described for hydralazine (Shepherd et al., 1981) and more recently reported (Doll and Hein, 2017) in cryopreserved human hepatocytes for the same probe drug (sulfamethazine).

Hydralazine *N*-acetylation was both time- and concentration-dependent *in situ* in cryopreserved human hepatocytes. Cryopreserved hepatocytes with rapid, intermediate, and slow

DMD#78543

acetylase genotypes produced the most, moderate, and least amount of MTP respectively. Thus both the *in vitro* and *in situ* results in cryopreserved human hepatocytes support the tri-modal model of hydralazine acetylation. An important finding during the *in situ* studies was the instability of hydralazine in most growth media. We conducted HPLC analysis of hydralazine in different types of media and found hydralazine to be unstable in all media tested and only stable in PBS. Therefore, after plating hepatocytes in the normal growth media for 48 hours, we cultured the hepatocytes in PBS + dextrose when incubating them with hydralazine to ensure that the cells were receiving the appropriate concentration of hydralazine.

Our results clearly document NAT2 genotype-dependent *N*-acetylation of hydralazine in human hepatocytes, suggesting that hydralazine efficacy and safety could be improved by NAT2 genotype-dependent dosing strategies. More specific dosing strategies, particularly in epigenetic clinical trials, could facilitate maximal therapeutic benefit from hydralazine.

DMD#78543

### **Acknowledgements**

We thank Timothy Moeller and Bioreclamation IVT (Baltimore, MD) for their valuable contributions. We thank Samantha Carlisle, Raul Salazar-González and Marcus Stepp for their review and suggestions to improve the manuscript.

### **Authorship Contributions**

*Participated in research design:* Allen, Doll, and Hein.

*Conducted experiments:* Allen and Doll

*Contributed new reagents or analytic tools:*

*Performed data analysis:* Allen, Doll, and Hein

*Wrote or contributed to the writing of the manuscript:* Allen, Doll and Hein

DMD#78543

## References

Arce C, Perez-Plasencia C, Gonzalez-Fierro A, et al. (2006) A proof-of-principle study of epigenetic therapy added to neoadjuvant doxorubicin cyclophosphamide for locally advanced breast cancer. *PLoS One* 1:e98

Candelaria M, de la Cruz-Hernandez E, Taja-Chayeb L, et al. (2012) DNA methylation-independent reversion of gemcitabine resistance by hydralazine in cervical cancer cells. *PLoS One* 7(3):e29181

Candelaria M, Gallardo-Rincon D, Arce C, et al. (2007) A phase II study of epigenetic therapy with hydralazine and magnesium valproate to overcome chemotherapy resistance in refractory solid tumors. *Ann Oncol* 18(9):1529-1538

Castillo-Aguilera O, Depreux P, Halby L, Arimondo PB, Goossens L (2017) DNA Methylation Targeting: The DNMT/HMT Crosstalk Challenge. *Biomolecules* 7(1) doi:10.3390/biom7010003

Chuang JC, Yoo CB, Kwan JM, et al. (2005) Comparison of biological effects of non-nucleoside DNA methylation inhibitors versus 5-aza-2'-deoxycytidine. *Mol Cancer Ther* 4(10):1515-1520

Cohn JN, McInnes GT, Shepherd AM (2011) Direct-acting vasodilators. *J Clin Hypertens* 13(9):690-692

DMD#78543

Coronel J, Cetina L, Pacheco I, et al. (2011) A double-blind, placebo-controlled, randomized phase III trial of chemotherapy plus epigenetic therapy with hydralazine valproate for advanced cervical cancer. Preliminary results. *Med Oncol* (Northwood, London, England) 28 Suppl 1:S540-546

Doll MA, Hein DW (2001) Comprehensive human NAT2 genotype method using single nucleotide polymorphism-specific polymerase chain reaction primers and fluorogenic probes. *Anal Biochem* 288(1):106-108

Doll MA, Hein DW (2017) Genetic heterogeneity among slow acetylator N-acetyltransferase 2 phenotypes in cryopreserved human hepatocytes. *Arch Toxicol* 91(7):2655-2661

Doll MA, Salazar-Gonzalez RA, Bodduluri S, Hein DW (2017) Arylamine N-acetyltransferase 2 genotype-dependent N-acetylation of isoniazid in cryopreserved human hepatocytes. *Acta Pharm Sin B* 7(4):517-522

Dueñas-Gonzalez A, Coronel J, Cetina L, Gonzalez-Fierro A, Chavez-Blanco A, Taja-Chayeb L (2014) Hydralazine-valproate: a repositioned drug combination for the epigenetic therapy of cancer. *Expert Opin Drug Metab Toxicol* 10(10):1433-1444

Garces-Eisele SJ, Cedillo-Carvallo B, Reyes-Nuñez V, et al. (2014) Genetic selection of volunteers and concomitant dose adjustment leads to comparable hydralazine/valproate exposure. *J Clin Pharm Ther* 39(4):368-375

DMD#78543

Gonzalez-Fierro A, Vasquez-Bahena D, Taja-Chayeb L, et al. (2011) Pharmacokinetics of hydralazine, an antihypertensive and DNA-demethylating agent, using controlled-release formulations designed for use in dosing schedules based on the acetylator phenotype. *Int J Clin Pharmacol Ther* 49(8):519-524

Graca I, Sousa EJ, Costa-Pinheiro P, et al. (2014) Anti-neoplastic properties of hydralazine in prostate cancer. *Oncotarget* 5(15):5950-5964

Hein DW (2009) N-acetyltransferase SNPs: emerging concepts serve as a paradigm for understanding complexities of personalized medicine. *Expert Opin Drug Metab Toxicol* 5(4):353-366

Hein DW, Doll MA (2017) Role of the N-acetylation polymorphism in solithromycin metabolism. *Pharmacogenomics* 18(8):765-772

Magee LA, Cham C, Waterman EJ, Ohlsson A, von Dadelszen P (2003) Hydralazine for treatment of severe hypertension in pregnancy: meta-analysis. *BMJ* 327(7421):955-60

McDonagh EM, Boukouvala S, Aklillu E, Hein DW, Altman RB, Klein TE (2014) PharmGKB summary: very important pharmacogene information for N-acetyltransferase 2. *Pharmacogenet Genomics* 24(8):409-25

DMD#78543

Segura-Pacheco B, Perez-Cardenas E, Taja-Chayeb L, et al. (2006) Global DNA hypermethylation-associated cancer chemotherapy resistance and its reversion with the demethylating agent hydralazine. *J Trans Med* 4:32

Shepherd AM, McNay JL, Ludden TM, Lin MS, Musgrave GE (1981) Plasma concentration and acetylator phenotype determine response to oral hydralazine. *Hypertension* 3(5):580-585

Singh V, Sharma P, Capalash N (2013) DNA methyltransferase-1 inhibitors as epigenetic therapy for cancer. *Curr Cancer Drug Targets* 13(4):379-399

Singh N, Dueñas-Gonzalez A, Lyko F, Medina-Franco JL (2009) Molecular modeling and molecular dynamics studies of hydralazine with human DNA methyltransferase 1. *ChemMedChem* 4(5):792-799

Spinasse LB, Santos AR, Suffys PN, Muxfeldt ES, Salles GF (2014) Different phenotypes of the NAT2 gene influences hydralazine antihypertensive response in patients with resistant hypertension. *Pharmacogenomics* 15(2):169-178

Tampe B, Tampe D, Zeisberg EM, et al. (2015) Induction of Tet3-dependent epigenetic remodeling by low-dose hydralazine attenuates progression of chronic kidney disease. *EBioMedicine* 2(1):19-36

Weber WW, Hein DW (1985) N-acetylation pharmacogenetics. *Pharmacol Rev* 37(1):25-79

DMD#78543

## Footnotes

This study was partially supported by United States Public Health Service National Institutes of Health grants [R25-CA134283 and P20-GM113226].

## Legends for Figures

Fig. 1: HPLC separation of hydralazine and MTP.

Fig. 2. Recombinant human NAT1 and NAT2 Michaelis-Menten kinetic constants for hydralazine. Scatter plots illustrate data from three independent measurements with mean shown by horizontal line. The apparent  $K_m$  for hydralazine was significantly ( $p=0.0016$ ) higher for recombinant human NAT1 ( $456 \pm 57 \mu\text{M}$ ) than NAT2 ( $20.1 \pm 8.8 \mu\text{M}$ ). The apparent  $V_{\text{max}}$  for hydralazine *N*-acetylation was significantly ( $p=0.0245$ ) lower for recombinant NAT1 ( $72.2 \pm 17.9$  nmoles acetylated/min/mg protein) than NAT2 ( $153 \pm 15$  nmoles acetylated/min/mg protein).

Fig. 3. Hydralazine *N*-acetyltransferase activities *in vitro* in cryopreserved human hepatocytes from rapid, intermediate and slow NAT2 acetylators. Scatter plots illustrate hydralazine *N*-acetyltransferase activities *in vitro* in cryopreserved human hepatocytes from rapid ( $n=6$ ), intermediate ( $n=5$ ), and slow ( $n=5$ ) NAT2 acetylators. Hydralazine *N*-acetyltransferase activities differed significantly with respect to NAT2 phenotype at each concentration tested:  $1000 \mu\text{M}$  ( $p=0.0319$ );  $100 \mu\text{M}$  ( $p=0.002$ ); and  $10 \mu\text{M}$  hydralazine ( $p=0.0029$ ).

DMD#78543

Fig. 4. Hydralazine *N*-acetyltransferase activities *in vitro* in cryopreserved human hepatocytes among slow NAT2 acetylator genotypes. Scatter plots illustrate hydralazine *N*-acetyltransferase activities *in vitro* in cryopreserved human hepatocytes with *NAT2*\*5B/\*5B (n=5), *NAT2*\*5B/\*6A (n=6), and *NAT2*\*6A/\*6A (n=5) genotypes. Hydralazine *N*-acetyltransferase activities differed significantly with respect to slow acetylator NAT2 genotype ( $p < 0.001$ ).

Fig. 5. Concentration and time-dependent *N*-Acetylation of hydralazine in cryopreserved human hepatocytes *in situ*. Cryoplateable human hepatocytes were plated on collagen coated 12-well plates and allowed to attach. After 48 hours, plating media was removed and cells were washed, then grown with PBS+ dextrose containing (0-1000  $\mu\text{M}$ ) hydralazine for 12 hours. Top: Each data point illustrates mean  $\pm$  SD in cryopreserved human hepatocytes from 5 individual rapid, intermediate or slow acetylators. Bottom: Each data point illustrates mean  $\pm$  SD in cryopreserved human hepatocytes from 5 individual rapid acetylators.

Fig. 6. *N*-Acetylation of hydralazine *in situ* in cryopreserved human hepatocytes from rapid, intermediate and slow acetylators. Cryoplateable human hepatocytes were plated on collagen coated 12-well plates and allowed to attach. After 48 hours plating media was removed and cells were washed, then grown with PBS + dextrose containing 10  $\mu\text{M}$  or 100  $\mu\text{M}$  hydralazine for 12 hours. Scatter plots illustrate hydralazine *N*-acetylation rates in rapid (n=5), intermediate (n=5) and slow (n=5) acetylator cryopreserved human hepatocytes following incubation with 100  $\mu\text{M}$  (top) and 10  $\mu\text{M}$  (bottom) hydralazine. Hydralazine *N*-acetylation rates differed significantly among the rapid, intermediate and slow acetylator cryopreserved human hepatocytes at 10  $\mu\text{M}$  ( $p = 0.002$ ) and 100  $\mu\text{M}$  ( $p = 0.0015$ ) hydralazine.

DMD#78543

## Figures

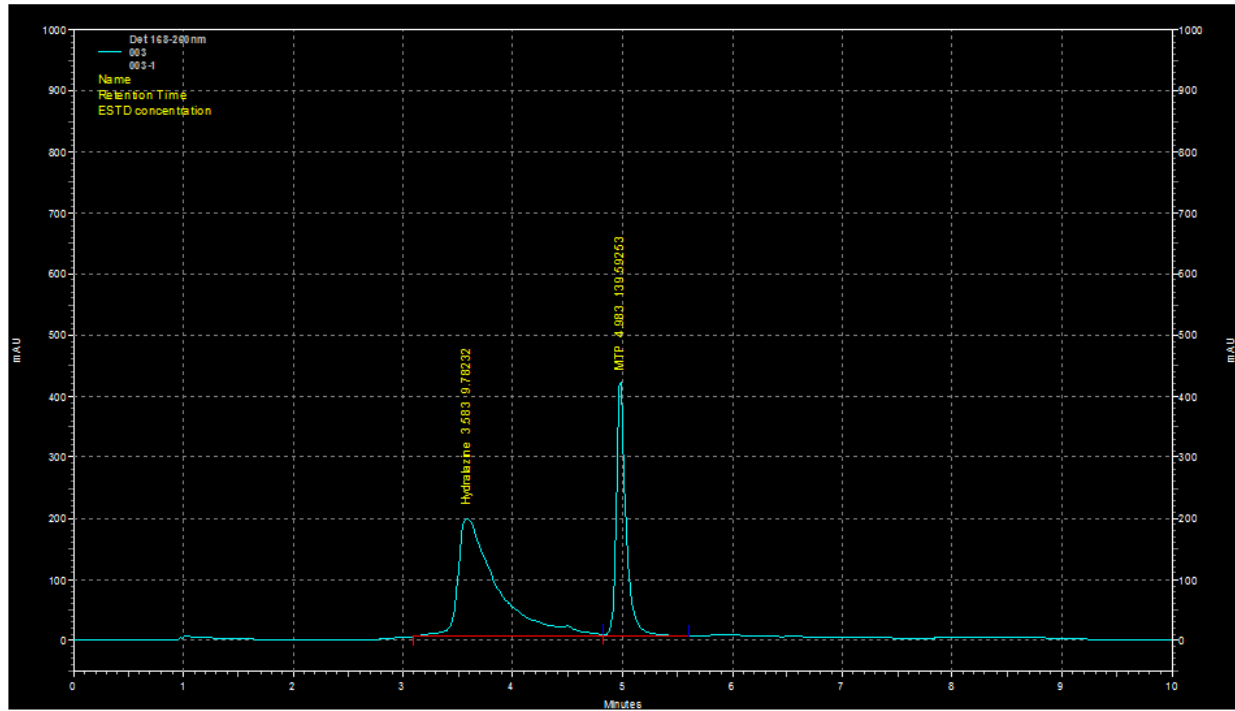


Figure 1

DMD#78543

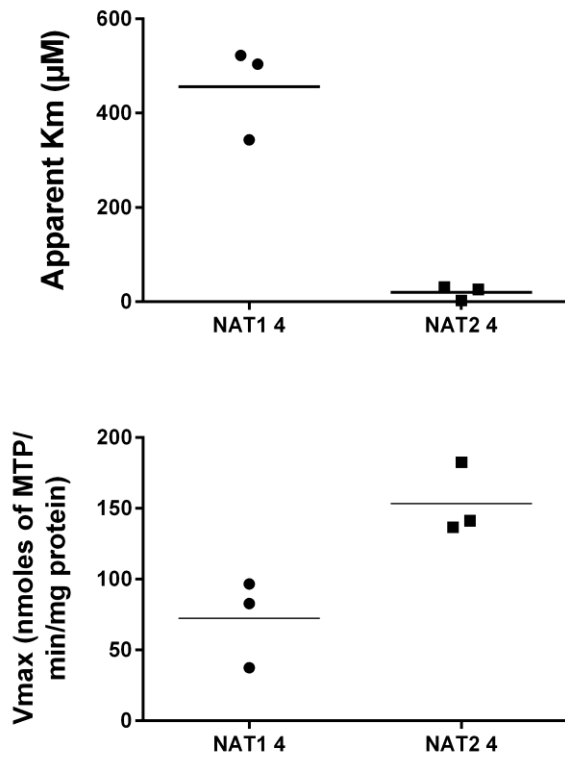


Figure 2

DMD#78543

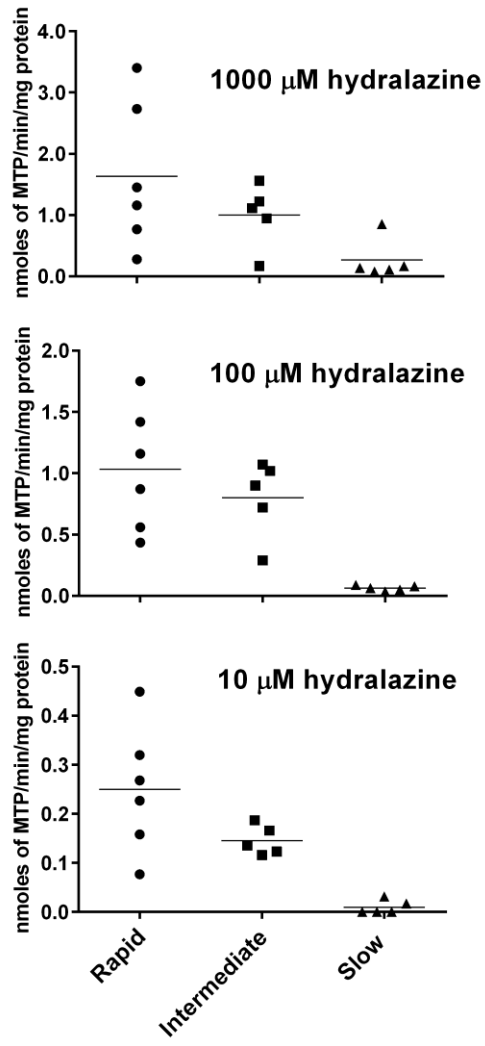


Figure 3

DMD#78543

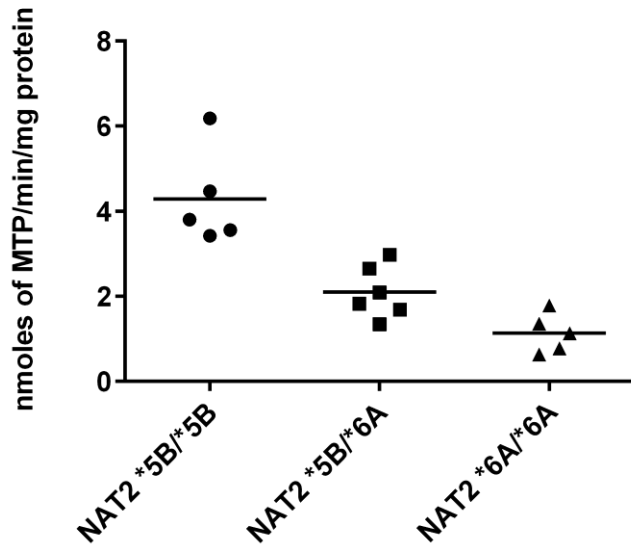


Figure 4

DMD#78543

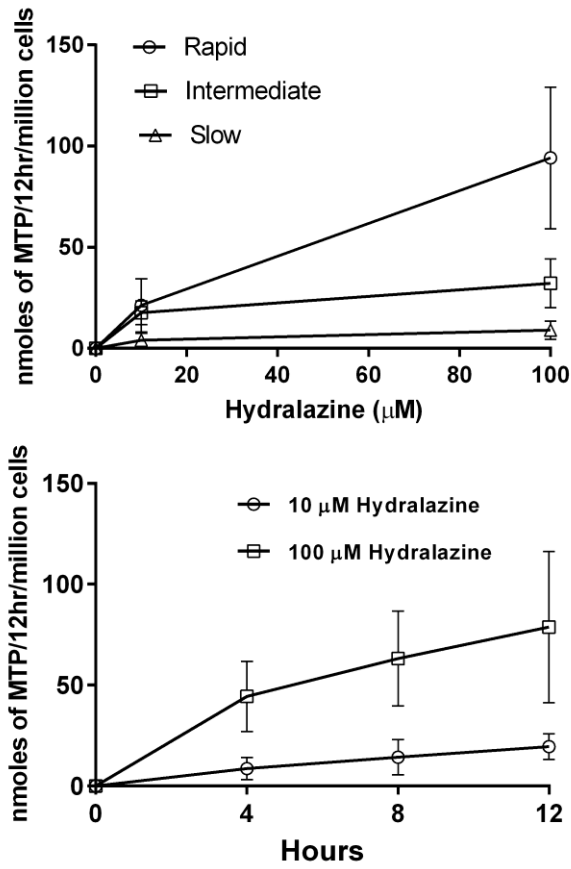


Figure 5

DMD#78543

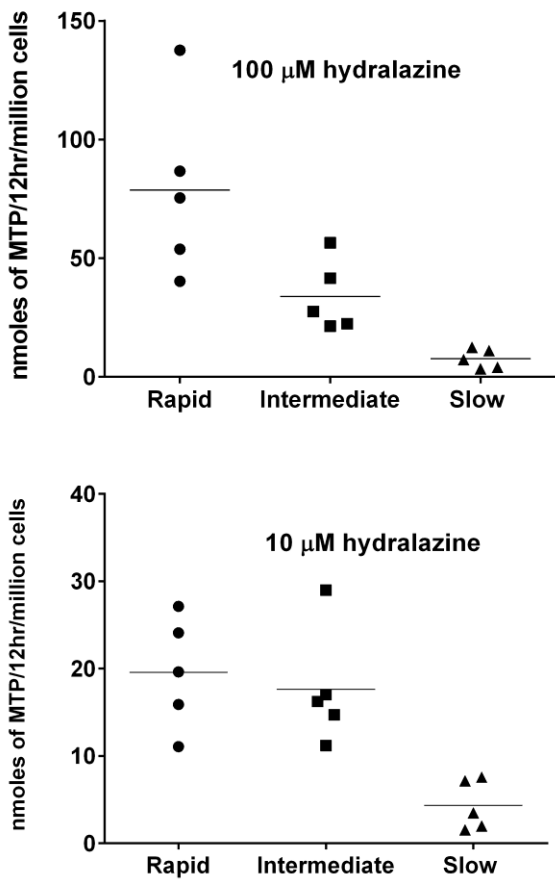


Figure 6